IOP Publishing Electron. Struct. 7 (2025) 023001 https://doi.org/10.1088/2516-1075/adcb7c

Electronic Structure

TOPICAL REVIEW

Electronic structure calculations for muon spectroscopy*

Stephen J Blundell[1], Miki Bonacci[2], Pietro Bonfà[3], Roberto De Renzi[3], Benjamin M Huddart[1], Tom Lancaster[4], Leandro M Liborio[5,**], Ifeanyi J Onuorah[3], Giovanni Pizzi[2], Francis L Pratt[6] and John M Wilkinson[6]

[1] Department of Physics, University of Oxford, Parks Road, Oxford OX1 3PU, United Kingdom
[2] Laboratory for Materials Simulations (LMS) and National Centre for Computational Design and Discovery of Novel Materials (MARVEL), Paul Scherrer Institut (PSI), CH-5232 Villigen PSI, Switzerland
[3] Department of Mathematical, Physical and Computer Sciences, University of Parma, Parco Area delle Scienze 7/A, 43124 Parma, Italy
[4] Department of Physics, Durham University, South Road, Durham DH1 3LE, United Kingdom
[5] Scientific Computing Department, Science and Technology Facilities Council, Rutherford Appleton Laboratory, Harwell Campus, Didcot OX11 0QX, United Kingdom
[6] ISIS Neutron and Muon Source, STFC Rutherford Appleton Laboratory, Chilton, Didcot OX11 0QX, United Kingdom
**Author to whom any correspondence should be addressed.

E-mail: leandro.liborio@stfc.ac.uk

Keywords: muon science, computational simulations, density functional theory, sustainable software, galaxy workflow management platform

OPEN ACCESS

RECEIVED
26 September 2024

REVISED
13 February 2025

ACCEPTED FOR PUBLICATION
10 April 2025

PUBLISHED
13 May 2025

Abstract

Muon spectroscopy has become a leading tool for the investigation of local magnetic fields in condensed matter physics, finding applications in the study of superconductivity, magnetism, ionic diffusion in battery materials, and numerous other fields. Though the muon yields quantitative information about the material, this can only be fully interpreted if the nature of the muon site and its stability is fully understood. Electronic structure calculations are of paramount importance for providing this understanding, particularly through a group of techniques that has become known as DFT+μ, density functional theory including the presence of the implanted muon. We describe how these electronic structure calculations can be used to underpin muon spectroscopy, and some examples of the science that follows from this, as well as some of the available software tools that are currently being developed.

1. Introduction

Muons are particles with a spin of $\frac{1}{2}$ that can be produced in either charge state, though in most of what follows we will be concerned with the positively charged muon. They can be embedded into condensed matter materials to serve as local probes of the surrounding magnetic environment. By measuring the muon's precession and relaxation, it is possible to gain insights into the muon's interactions with its surroundings. This experimental technique yields unique information about the static and dynamic properties of the material under study and has found wide application in many condensed matter physics studies [1–3]. (For a detailed review of the principles behind the experimental technique, see [4].) The remarkable features of the muon that enable these studies are that (i) beams of muons can be produced with full spin polarization, (ii) the muon spin is preserved in the implantation process (as discussed in section 2), and (iii) the direction of positron emission produced by the decay of the muon is determined by the spin orientation of the muon due to parity violation in the weak interaction [5], and hence the time dependence of the muon spin polarization can be recorded experimentally.

Because the gyromagnetic ratio of the muon ($\gamma_\mu = 2\pi \times 135.5\,\mathrm{MHz\,T^{-1}}$) is well known, the muon's magnetic coupling to its environment can be determined very accurately. However, to enable quantitative predictions, it is also necessary to know the site at which the muon implants. Moreover, the presence of a

* This article presents a summary of the state of the art of computational simulations for muon science. All authors have contributed equally to it.

charged ($q = +e$) 'impurity' spin inside the material will inevitably cause some local distortion; the degree and nature of this distortion needs to be quantified in order to ascertain the extent to which this might affect the properties being measured. Both of these aspects can be addressed using electronic structure calculations, as will be described in this article.

Density functional theory (DFT) methods had been used to study muonium (the complex μ^+e^-) in silicon [6], but the recent interest in DFT techniques applied to muon problems stems from calculations of muon sites in various ionic fluorides [7, 8]. Fluorides were chosen because the muon site can be identified by the distinctive experimental signature that arises from an F–μ–F state due to the coupling between the muon spin and the ^{19}F nuclear moments (and despite the lack of electronic magnetism in many ionic fluorides) [9]. The fluorine's high electronegativity makes it highly attractive to the positively charged muon, and the small ionic radius of fluoride allows the muon to sit very close to it. Moreover, ^{19}F (that occurs with 100% abundance) has nuclear spin $I = \frac{1}{2}$ and a large nuclear moment. The resulting experimental signature allows the muon–fluorine bond length to be measured accurately, therefore ionic fluorides were the obvious target systems to test the reliability of DFT methods in determining the muon site [7, 8], and have been used for quantifying the decohering effects of more distant nuclear spins in fluorides [10].

These investigations on fluorides have now been extended to many other systems [11], and the electronic structure techniques are often referred to as DFT+μ: DFT including the effect of the implanted muon. However, as will be described in this article, there are features concerning implanted states that can have profound implications. First, the muon mass is small, roughly one-ninth of the proton mass, and so quantum effects are significant, resulting in large zero-point energies and the possibility of diffusion between sites. Second, the implanted muon is sensitive to local properties and this makes DFT well suited to this problem, since calculations performed within a supercell can provide detailed information about local structure.

This paper is structured as follows. In section 2 we provide an overview of the muon spectroscopy technique, describing the types of problems that are amenable to study using muons. In section 3 we describe the range of different electronic structure techniques that can be applied to muon spectroscopy. In section 4 we describe the many different software tools that are currently available for performing μSR electronic structure calculations.

2. Muons and the μSR technique

The experimental technique involving muon implantation into samples is usually known as μSR, which stands for muon-spin rotation (referring to the Larmor precession of the muon spin in a static magnetic field) or muon-spin relaxation (referring to the analogue of T_1 processes in NMR whereby spin polarization returns to its equilibrium value). In either case, on implantation into a material, muons interact with their local environment before decaying into a positron (for μ^+), or an electron (for μ^-). The decay particle is emitted preferentially along the final spin direction, so that by monitoring the angular distribution of positron (or electron) emission, the time-dependence of the muon spin polarization can be inferred. Positively charged muons implant in an interstitial site, or bond to a molecular group, and are sensitive to the physics of nearby spin-polarised electron density and nuclear spins. In contrast, negatively charged muons implant close to the atomic nucleus and yield quite different information (and will be discussed in more detail in section 3.7). The technique requires the use of bulk samples because, in the case of the most often used 'surface muons' (muons produced from the stopped pions in the surface of a target), the muons are formed with energy 4 MeV and penetrate a few hundred micrometers into any material.

The production of muons in sufficient quantities for μSR experiments require a proton accelerator of a size beyond the capability of any single university group, and consequently they are housed at large international user facilities. Currently the main user programmes are operated at ISIS (UK), JPARC (Japan), PSI (Switzerland), and TRIUMF (Canada). The first two of these provide pulsed muon beams; the second two are sources of continuous muon beams. In pulsed muon beam experiments there are a large number ($\sim 10^3$) of muons arriving in a very intense pulse and the detection of positrons is timed with respect to the arrival of the pulse. In contrast, in continuous muon beam experiments a single muon is in the sample at any one time. This limits the data rate to a few tens of thousand muons per second, since the arrival of the following muon must be delayed so that its subsequent decay will not become confused with the decay of the preceding muon. Nevertheless, experiments with continuous muon beams allow for a superior time resolution (and hence resolution of high-frequency precession signals), which are instead limited in pulsed beam experiments by the finite width of the muon pulse. This delicate tradeoff between frequency resolution and data rate means that both pulsed and continuous muon beams have complementary advantages. In both cases, though, the density of muons in the sample at any one time is extremely low, so that muon–muon interactions can be neglected entirely.

μSR has been employed in a wide variety of areas of condensed matter physics and chemistry [1, 4]. It has found particular application in magnetism, where it has been used to measure the order parameter in magnetically ordered phases and study dynamics in spin glasses. It is very useful in studying frustrated magnetic systems in which there is no long-range order, but instead a fluctuating dynamical state. The ability of the muon to undergo spin precession in a static magnetic field (as might be found inside a magnetically ordered phase) or spin relaxation in a time-varying magnetic field (as might be found inside a magnetically fluctuating system) is key to the usefulness of the technique. In superconducting systems it is the ability of the muon to sense the field variations inside a superconducting vortex lattice that allows it to yield information about the magnetic penetration depth. Moreover, many systems exhibit a competition between magnetically ordered and superconducting ground states and this has led μSR to be very effective in mapping out the phase diagrams of new superconducting families, such as the iron-based superconductors (see e.g. [12]). The muon's sensitivity to small magnetic fields means that it can pick up the field from nuclear magnetism, and this has allowed it to be a probe of lithium ion diffusion in battery materials. On implantation, a muon can form a muonium (μ^+e^-) bound state which can mimic the behaviour of hydrogen, and this has led to the muon being used as an analogue of hydrogen for studies of its behaviour in semiconductors [13]. In chemical systems, muonium addition can create new radicals whose hyperfine constants and chemical kinetics can be measured [14]. Note here that the addition of muonium leads to a muoniated charge-neutral state. The term muoniated distinguishes the neutral state from the positively charged state formed by addition of a bare positive muon, which is labelled muonated. Altogether, these examples demonstrate the wide applicability of μSR to many science applications.

3. The role of simulations in μSR

3.1. Stopping site

In many systems, each muon will stop in the same crystallographic site on every implantation. In other systems, there could be more than one crystallographically distinct muon site if they turn out to have similar final energies. But how we do identify these sites? In some cases, the candidate muon sites can be assigned by an educated guess that uses experimental data, and sometimes their probability distributions can be modelled. For instance, in fluorides, the muon stopping site is found by measuring the distinct muon frequencies that originate in a F–μ–F state (see section 1). However, the number of examples where the muon site can be determined by experimental means alone is limited, and can be experimentally very costly, as was found in the case of MnSi [15]. There are other examples where a limited number of calculations were used to test potential muon stopping sites that had been proposed using available experimental information [16]. Finally, there is an approach where the position of the muon could be represented by a probability distribution across stopping sites, and the knowledge of the exact muon stopping site may not be necessary. If the goal is to measure a magnetic moment of a magnetic ion in a given structure, a Bayesian method can be applied to quantify the knowledge about the muon stopping site [17]. This knowledge is represented by assuming a certain distribution of muon sites in the unit cell, which can be expressed as a probability density function. This approach has been successfully tested in a number of examples [18, 19].

Given that none of the techniques described above can give a conclusive answer to the question of the muon stopping site, it is useful to have a methodology that can systematically explore and propose potential stopping sites when very little information is known about the system [20]. The recently developed DFT-based methods for finding the muon stopping sites improve on the methods described in the previous paragraph by using DFT simulations to provide a reliable set of potential stopping sites that are estimated using only theoretical means. In crystalline materials, DFT calculations assume that the crystal is periodic in all three dimensions. Hence, periodic boundary conditions are necessary to perform these calculations. Given that muons in a μSR experiment are implanted in an ultra-dilute limit, the calculations are carried out in a supercell (comprising multiple unit cells and a single muon) to ensure that boundary conditions do not lead to muon–muon interactions. Many of these methods begin by generating a set of muonated crystalline structures where a muon is placed in a random initial position within a supercell of the target material. These structures are then relaxed by allowing the muon and/or the atoms in the crystal to adjust their positions through repeated iterations, until the forces acting on them fall below a certain threshold. The total energy of the final relaxed configuration is then evaluated. The muon's charge state is determined by the overall charge of the defect (with $+1$ for diamagnetic and neutral, and zero for paramagnetic states), which is initially fixed. For the diamagnetic case, a uniform, smeared-out Hartree-like compensating charge is added to the supercell to maintain overall neutrality. The final charge state of the impurity is determined after the structure has been relaxed. The geometry optimization is repeated for several other randomly chosen initial muon sites. The site with the lowest total energy after relaxation is often taken to be the most likely muon site and provides an estimate of the structural distortion caused by the muon. This process generally results in multiple candidate

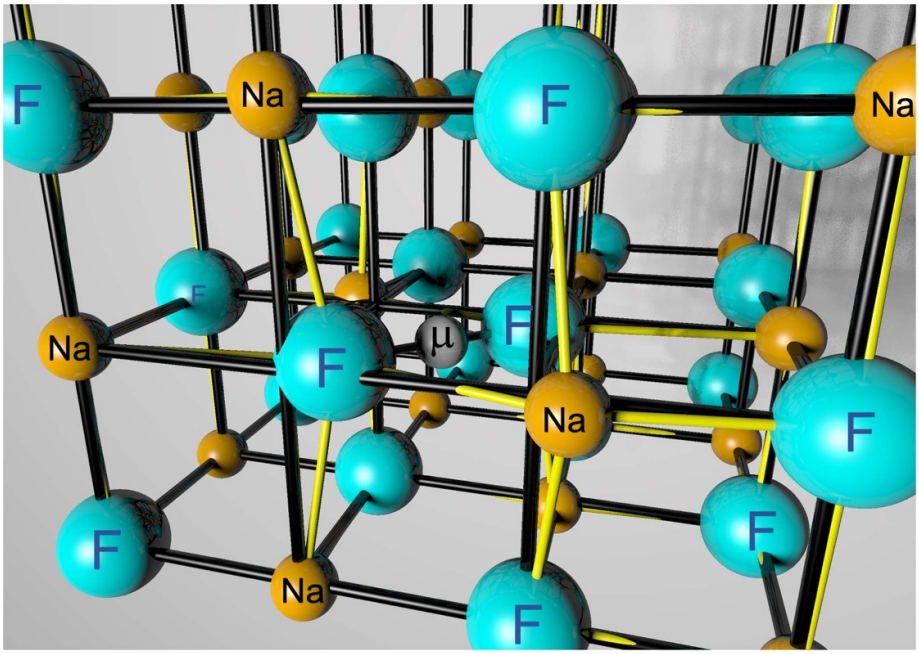

Figure 1. The muon site in NaF calculated using DFT+μ, together with the muon-induced distortion. The thick black lines show the nearest Na–F distances in the undistorted structure, and those coloured yellow show the corresponding distances in the muon-containing structure. The muon pulls in two fluorine anions to make the F–μ–F state and pushes two nearby sodium cations away.

muon sites. These sites are then grouped into clusters of roughly equivalent locations. This clustering is most efficiently achieved by utilizing the underlying symmetry of the unperturbed crystal structure, along with assumptions about the nature of the distortion and the energy ranges of the sites likely to be realized.

Section 4 presents some of the software tools that are currently available for performing this systematic analysis, and more detailed discussions of the nature of the stopping site problem can be found elsewhere [11].

3.2. Distortion caused by the muon

As stated in section 3.1, the methods for finding the muon stopping sites generate a set of muonated crystalline structures. DFT geometry relaxations are performed on these structures, and the muon and its nearby atoms in the supercell are allowed to relax. Hence, together with the mon stopping site, one also obtains the effect of the presence of the muon on nearby atoms and ions. For example, consider the compound sodium fluoride (NaF) which adopts the cubic NaCl crystal structure, a face-centered cubic lattice with a two-atom basis (with Na^+ at $(0,0,0)$ and F^- at $(0,0,\frac{1}{2})$) and lattice parameter $a = 0.559$ nm, so that the nearest fluorine–fluorine distance is $a/\sqrt{2} = 0.395$ nm. The muon implants at $(0,\frac{1}{4},\frac{1}{4})$, as shown in figure 1, and pulls in the two nearest fluorine ions towards itself, so that the muon–fluorine distance is 0.120 nm [10], close to the hydrogen–fluorine distance 0.114 nm in the bifluoride ion [21]. This means that the fluorine–fluorine distance (along the direction through the muon) is now 0.240 nm, substantially lower than the equilibrium value $a/\sqrt{2} = 0.395$ nm. The nearest sodium cations are similarly pushed away from the muon, resulting in a sodium–sodium distance (along the direction through the muon) of 0.462 nm, substantially higher than the equilibrium value $a/\sqrt{2} = 0.395$ nm. The distortive effect of the muon has the greatest effect on the nearest ions, and the effect decreases sharply as you consider more distant ions which are hardly affected by the presence of the muon.

The distorting effect of the muon can sometimes have significant consequences, and a good example of this is found in quantum spin ice materials containing Pr^{3+} ions. Here, the basic physics is highly dependent on the crystal field, which is in turn determined by the arrangement of anions surrounding the lanthanide cation. Without the muon, the Pr^{3+} ion is coordinated by eight oxygen anions and adopts a doublet crystal field ground state, resulting in an effective spin-$\frac{1}{2}$ moment. However, DFT+μ calculations imply that the presence of the muon (the site is identified as $(-0.013, 0.047, 0.203)$) distorts the local symmetry around nearby Pr^{3+} ions. The largest effect is found to be an anisotropic distortion, with one Pr–O bond strongly rotated (bent) and another significantly extended. This splits the doublet ground state on local Pr cations, which then possess single ground states which can become hyperfine enhanced. The model which describes

this effect (involving DFT+μ calculations of the distortion and crystal field calculations of the resulting Pr environments) produces quantitative agreement with the temperature dependence of the μSR data from experiment, demonstrating the validity of this approach [22]. This effect is particularly important in these materials, since Pr^{3+} has a non-Kramers ground state which is particularly vulnerable to electrostatic perturbations.

There are many cases where the evaluation of the distortion caused by the muon impurity is important in showing that it does *not* significantly affect its local crystalline or electronic environment. An example is in the class of superconductors that have been proposed to show time-reversal symmetry breaking on the basis of muon measurements. Here the computation of muon sites across several materials demonstrates that the muon does not cause a significant perturbation to the local crystal environment, and that the muon energy level is buried deep beneath the Fermi energy of the superconductor, such that it should be expected to have only very limited influence on the physics [23].

3.3. Quantum effects and tunnelling

An assumption in many computations of muon stopping states is that the muon can be treated as a classical point particle. However, such an assumption is often questionable [4]. The muon is nine times lighter than hydrogen (and in DFT is usually treated as if it were a light isotope of hydrogen) and quantum zero-point motion (ZPM) effects, such as anharmonicity, are known to be significant for particles with such small masses. In practice, we might expect quantum effects to lead to changes in the calculated energy and stability of the muon site, owing to a relatively large muon zero-point energy (ZPE), along with possible delocalization of the muon and quantum tunnelling [24].

To account for quantum effects, approximation schemes generally fall into two classes. The first are adiabatic single-particle methods where we solve a single-particle Schrödinger equation for an effective muon potential obtained by adiabatically decoupling the muon and nuclear positions (for either a very fast or a very slow muon). The second set of approaches are the harmonic multi-particle methods. These describe quantum-entangled muon–nuclear ZPM, but assume purely harmonic muon–nuclear interactions. Alternatively, a more recent trend has been towards using *ab initio* path-integral molecular dynamics (PIMD) simulations to capture related quantum-hydrogen effects with some success. This is a numerically exact method that can describe the fully anharmonic multi-particle nuclear ZPM, which is known to be important for hydrogen. A recent test case for these methods was that of α-N_2 [24]. Here, both adiabatic and harmonic approaches were shown to be inconsistent and a PIMD computation was required to capture the correct physics. Finally, a compromise between accuracy and computational efficiency can be obtained with two different strategies for treating muon states in crystals. The stochastic self-consistent harmonic approximation includes them in the phononic contribution to the total energy [25–27]. It can account for anharmonicity and includes quantum and, possibly, thermal fluctuations. A second option is to jointly solve the muon-electron problem using two-component DFT, a method widely used to compute positron states in matter recently extended to the case of positive muons [28, 29] with promising results. In this method, the muon and the electrons are treated using DFT.

In order to study the possibility of quantum diffusion or tunnelling between candidate sites, transition-state searches provide a practical route to the computation of potential barriers. An illustrative example of this in the context of μSR is in 1 T–TaS_2 [30] where the low energy barrier between three of the four candidate muon sites, along with sizeable ZPEs, was suggested to lead to muon delocalization across these positions.

3.4. Diffusion of muons

Since the implanted muon is often used to probe the diffusion of mobile ions, e.g. in studies of energy materials [31], it is important to know whether the muon is a straightforward static probe or whether the muon is itself diffusing, which makes quantitative interpretation of the diffusion of the other mobile ionic species in the system much harder to extract. As a hydrogen-like particle, the potential map for the positive muon will follow that of a corresponding H^+ ion with matching minimum energy sites and potential barriers between potential minima. If the potential barriers are relatively small, then the quantum delocalisation and tunnelling covered in the previous section will be important. On the other hand, if the barriers are sufficiently large, then diffusion can be treated in terms of classical activated diffusion models. In this case, the light mass of the muon will enhance the classical diffusion rate in two ways. Firstly, the large zero-point energy of the muon will reduce the effective barrier height E_A compared to that seen by a heavier particle of the same charge and secondly, the enhanced vibrational frequency will increase the attempt frequency ν_0 in the Arrhenius model for thermally activated hopping, defined by the equation $\nu = \nu_0 \exp(-E_A/k_B T)$.

Electronic structure calculations have great potential for allowing these factors to be evaluated, so that the thermal threshold for the onset of muon diffusion in a particular system could in principle be predicted.

This would involve making a transition-state analysis of the potential along the diffusion path and a vibrational analysis of the muon around its equilibrium site. One recent example of this approach is a study of muon diffusion in the cubic perovskite oxide $KTaO_3$ [32]. Although such calculations would clearly be very helpful in planning and interpreting muon experiments aiming to study ionic diffusion, they have yet to be fully exploited. However, it should be noted that all the computational methods needed are readily available and this is likely to be an area of increasing importance, given the current rapid growth in research on battery materials using muons.

3.5. Treatment of muon–electron hyperfine coupling (HFC) with simulations

In many of the applications of μSR, the modelling of the muon–electron HFC is important for identifying different muonated and muoniated species [33], probing the muon's local environment [34] and studying the structure and dynamics of those species [35].

The required HFC modeling is based on DFT simulations, which require the accurate representation of the wavefunctions for the valence and core electrons. When DFT is implemented using pseudopotentials, valence wavefunctions may become smoothed near the nucleus and the associated calculations may lead to a non-physical spin density in the core-region. This can be corrected by using the projected augmented wave method [36], which is typically combined with the frozen-core approximation. The resulting core wavefunctions may have issues with the spin-core polarisation that may affect the calculation of the spin density at the nucleus [37, 38]. When the DFT implementation is in an all-electron, localised basis-set code, one of the main sources of error for the HFC is the quality and completeness of the basis set. The localised basis set representation of an *s* orbital comprises Gaussian functions that have zero slope at the origin. This reduces the values of the wavefunction, electron, and spin density at the nucleus compared to those of hydrogenic orbitals [39]. These issues are compounded by another problem that can affect the modelling of the HFC, namely the treatment of the electronic correlation, which may result in errors of up to 100% [40] for the HFC.

In the particular case of the muon–electron HFC in muonium, the level of precision of current DFT implementations is sufficient to determine the scanning range required to carry out a muon avoided-level crossing (ALC) experiment [41], or for identifying the molecular structure of simple muoniated radicals [35]. However, there are an increasing number of studies where the current level of precision (around 15%–20% of the experimental values [34, 35, 41]) presents a significant problem. This is the case, for example, in biological samples [35] or complex catalysts [42]. In these systems, there is considerable merit in measuring in solution, where narrow, and often weak, lines allow multiple distinct radical sites to be properly identified. Unfortunately, without high-precision calculations of the HFC, these lines can be a challenge to locate experimentally and measure, while interpretation of the final ALC spectra depends critically on the quality of the calculations.

Hence, improving the simulations of the muon–electron HFC could enable the accurate assignment of the experimental spectra of a complex system, and the development of a predictive tool for experiment planning.

3.6. Photo-excited μSR

One of the growing areas of μSR research is in photo-excited experiments. These involve illuminating the sample using a laser beam, and observing how the excited state affects the electronic structure around the muon by looking at how the spin polarisation of muons in muonium states evolve in time [43, 44]. This has found applications in semiconductor studies, particularly in the study of photovoltaics and muonium chemistry [45–48]. Despite it being possible to use DFT to predict the muon sites of the compounds in question [20], modelling the excited states of these is more challenging due to the infamous bandgap problem in DFT [49].

The Bethe–Salpeter equation (BSE) has been successful in the modelling of excited states in compounds, and goes some way to fixing the bandgap problem in DFT by perturbatively treating the electron–hole coupling in photo-excited states [50]. Guided by these successes, there have been attempts to model experiments by combining DFT (using Gaussian basis sets) with the BSE [51]. These calculations are computationally intensive, as the finite-size effects of including the muonium in the host compound often creates a surface conducting state, so that the calculations have to be done using very large supercells.

Currently, a team from STFC have a codebase (a modified version of Xatu [52]) which is able to calculate the excitations of a compound given the band structure calculated with DFT. They have been able to use this to predict the electron–hole coupling in excited muonium states, and calculate the absorption spectrum resulting from these excitations. The main limitations of these calculations is the computational effort

required in computing these states, which has so far limited the class of materials studied to simple semiconductors.

3.7. Negative muon experiments

3.7.1. Muonic x-ray elemental analysis

Negative muons can be thought of as 'heavy electrons' that, when implanted in a sample, replace an electron in the outer shell of an atom and then decay through its corresponding energy states. Each energy transition on this path produces an x-ray characteristic of the atom that absorbed the muon and creates a spectrum that identifies the atomic species, forming the basis for muonic x-ray elemental analysis. The technique is so sensitive that even atoms as light as Li can be detected [53]. Muonic x-rays are intense enough to pass through the sample material from the deep interior and can be easily detected once outside. Moreover, the depth of muon implantation in the sample can be controlled by adjusting the incident muon momentum. Hence, the combination of depth control, high element sensitivity and high-energy muonic x-ray emissions allows for investigation of elemental composition from micrometres to centimetres below the sample surface [54, 55]. Muonic x-ray elemental analysis has been used in diverse scientific areas, such as for studying meteorites [56] or functional nanomaterials [57], but one of the main applications of the technique is in the area of cultural heritage [58]. Muonic x-ray elemental analysis can be an important step in the study of archaeological artefacts. The knowledge of the atomic composition of a given artifact give scientists, historians, and curators tools for making assumptions about the manufacturing process of the object, its origins and the historical and material context of the populations who manufactured it.

While there exist tabulated databases of muonic atom x-ray frequencies [59], it is also important to have software tools that could be used to aid with muon elemental analysis. The Muon Spectroscopy Computational Project (MSCP) is a software development project based at STFC (see section (4.3)) that has been developing `MuDirac` [60], a modern, open-source, sustainable software tool that is being used to aid in muonic x-ray elemental analysis via the computation of muonic x-ray spectra. `MuDirac` can compute muonic atom transition energies, and probabilities for x-ray lines, up to precisions on the order of the keV, accounting for the effects of finite nuclear size, vacuum polarizability and electronic shielding. At the moment, the MSCP is developing the next version of `MuDirac`, which will be able to calculate the intensities of these muonic x-rays and improve its ability to perform quantitative elemental analysis efficiently.

3.7.2. μSR with negative muons

The use of negatively charged muons for μSR is less widespread than regular μSR using positive muons. However, there are some key advantages for negative muons. Firstly, the negative muon is captured within an atom in the sample to make a muonic atom. The position of the muon probe is then very clear, being at the known lattice site, rather being at a less well determined interstitial site, as would be the case for a positive muon. The muon in the muonic atom does not diffuse and the muonic atom is very stable chemically, so the negative muon can be a very good local probe. The muon lifetime depends on the probability of nuclear capture within the muonic atom, which can differ widely between elements. This can allow signals from muons within different probe atoms to be distinguished.

The disadvantages of negative muon μSR are that only around 1/6 of the muon polarization is retained during the capture cascade from the outer shell states to the deep inner orbit of the ground state. If the nucleus of the capture atom has spin, the muon will be less useful as a probe of its surroundings as this nuclear spin will dominate the local field seen by the muon. The muon data rates can be very low unless a high momentum beam is used, which requires a relatively large sample mass compared to μSR with positive muons. Also, the different muon lifetimes for different atoms means that the measured signals can be very complex. Some progress has been made recently with data analysis methods that are tailored more closely to the characteristics of negative muon μSR [61].

From a computational point of view, having the known muon site is helpful, but account needs to be taken of structural relaxation around the muon site due to the altered charge state and valence change of the atom, since the atom is effectively transmuted from atomic number Z to $Z-1$ by the presence of the muon in a deep orbit close to the nucleus. In the case of a semiconductor, this can be likened to n-type doping. Electronic structure computations for negative muon μSR are still at an early stage. A DFT study of MnO found bond length changes of up to 20% when the negative muon is present. The distortion from high symmetry was found to be necessary to explain the measured finite local field in the magnetically ordered state [62]. Further analysis of negative muon μSR for MgH_2 showed that the nuclear dipolar field at the muonic Mg site was correctly reproduced by the DFT when the local distortion was taken into account [62]. Altogether, these first steps in DFT for negative muons have given some very promising results and this is clearly something that should be done in conjunction with any negative μSR experimental studies.

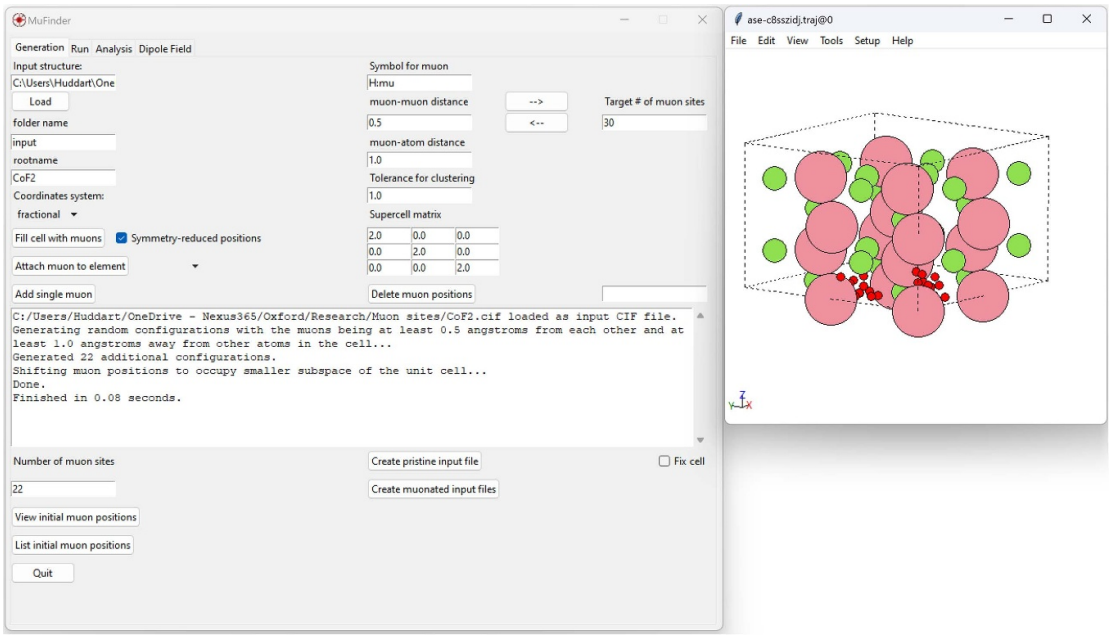

Figure 2. A screenshot of the MuFinder program [67], demonstrating initial muon position generation. Left: the main GUI window. Right: initial muon positions in a $2 \times 2 \times 2$ supercell of CoF_2 visualized using ASE's GUI, which is built into the program.

4. Software tools for μSR calculations

Several software tools are available to treat the different problems involved in interpreting muon measurements.

4.1. MUESR/UNDI

MUESR [63] is a small python library to quickly compute the local field at the muon sites by approximating (localized) magnetic moments of electronic origin as classical dipoles located at the atomic sites. The code takes as input a lattice structure and a magnetic order defined with the propagation vector formalism, and provides convenient routines to compute the dipolar field in real space with the Lorentz approach [4]. The core functionalities are implemented in C (which results in significant speed improvements), while the user can interact with the program through high-level APIs using the Python programming language. The code handles both commensurate and incommensurate magnetic orders and includes a dedicated algorithm to speed up the computation of the field distributions of helical phases [64].

UNDI [65] is Python library to compute the polarization function of a muon interacting with a set of neighbouring nuclei at the quantum level. The selected set of particles is described by a spin Hamiltonian, which includes the dipolar couplings between the various particles and the effect of electric field gradients (EFG) at quadrupolar nuclei. A Zeeman contribution and user-defined terms can also be specified. The code can compute the exact time evolution of the muon spin when the Hilbert space is sufficiently small, but it is most often used to obtain an approximate polarization function which neglects the inter-nuclear dipolar interaction. The procedure introduced by Celio [66] makes the problem computationally efficient and the approximation is generally well justified in light of the weaker dipolar interactions that occur among the nuclei, owing to the longer distances and the smaller gyromagnetic factors when compared to the dipolar interactions involving the muon.

4.2. MuFinder

MuFinder [67] is a graphical user interface (GUI)-based program that allows users to calculate muon stopping sites using DFT and the structural relaxation approach. The MuFinder GUI (figure 2(left)) comprises four tabs, each facilitating a step in the muon site calculation workflow, with the user expected to work through these from left to right. Given a crystal structure, candidate structures consisting of a muon embedded in the structure are generated; the only input required is a CIF file describing the structure. These structures are then relaxed using the plane-wave basis-set electronic structure code CASTEP [68], with these calculations being run either locally or remotely on a high-performance computing (HPC) cluster from within the GUI. Tools are provided to analyze the results of these calculations. MuFinder also allows the

calculation of the dipolar magnetic field at the muon site by providing an interface to the MUESR Python library [63].

MuFinder makes use of the atomic simulation environment (ASE) [69] library to manipulate, analyze and visualise atomic structures, enabling, for example, the evaluation of muon-induced distortions to the host crystal. We note that, while only the CASTEP electronic structure code is currently supported, ASE provides Python wrappers for a large number of codes including other plane-wave basis-set DFT codes such as Quantum ESPRESSO [70] and Gaussian based electronic structure codes such as Gaussian [71] and the DFT-based tight binding code DFTB+ [72], allowing the possibility for a wider variety of electronic structures codes to be supported in the future.

4.3. The MSCP and the Galaxy platform

The MSCP[7] is a joint project between the Scientific Computing Department and the Muon Group at the Science and Technologies Facilities Council (STFC) in the UK. The purpose of the MSCP is to develop sustainable, user-friendly software for the interpretation μSR experiments. Some examples of the software tools developed by the MSCP are `pymuon-suite` [20], which can be used for finding the potential stopping sites of muons in crystalline periodic systems; `muspinsim` [73], which simulates the spin dynamics of a system of a muon plus other spins, namely electrons and atomic nuclei; and `MuDirac` [60], which model muonic atoms. These tools are being developed as a new resource for the muon user community, following sustainable software engineering practices to ensure their longevity. They have been tested in different physical systems and they form part of the new set of computing simulations resources that are now being used to interpret μSR experiments. To improve the usability of the MSCP's tools, and further engage with the μSR community, the tools have been included in the Galaxy platform.

Galaxy [74] is an open source web platform for FAIR data analysis and workflow management. It was developed in 2005 to support genome analysis within the bioinformatics community. However, over time interest in using Galaxy has extended outside of the bioinformatics field, and it is now being used in areas such as astrophysics, climate science and materials science. No specific programming knowledge is required to use the Galaxy tools and workflows. Galaxy also supports visualisations and interactive tools: users can visualise their results, or run Jupyter notebooks, within the Galaxy interface. When a user runs a tool or workflow, the inputs and outputs are all stored in a 'history', which contains information about exactly which tools were run and what parameters were used in each one. The history then becomes a self-contained unit that describes exactly how to reproduce the results. This is exceptionally useful from a FAIR perspective, especially as histories and workflows can be shared with other users or made public[8]. Galaxy tools are open source and can be browsed via the Galaxy Tool Shed[9]. This enables global sharing of reproducible workflows without the requirement to be able to access exactly the same resources.

The MSCP, is developing the Galaxy instance `materialsgalaxy`[10], which is being used to foster the use of computational modelling for interpreting muon experiments; to increase the uptake and distribution of the software tools; to improve the transparency and reproducibility of the research results and as a simple GUI for the MSCP's tools. `muspinsim` has been installed in `materialsgalaxy` together with `pymuon-suite`, for which a detailed tutorial is available in the Galaxy Training Network[11]. Figure 3 shows the Galaxy's main GUI.

4.4. AiiDA workflows for muons

The `aiida-muon` package [75, 76][12] implements an automated workflow for the identification of muon sites, the evaluation of hyperfine constants and the computation of nuclear spin relaxations. It relies on the functionalities provided by the AiiDA (Automated Interactive Infrastructure and Database for Computational Science) framework [77–79], which integrates an interface to directly interact with HPC facilities and deploys database technology for the storage and preservation of computational results, with ease of retrieval for reproducibility. The current implementation exploits the `aiida-quantumespresso` plugin to perform all DFT based simulations and it utilizes various libraries for computing the muon interactions (MUESR and UNDI, see section 4.1) and for handling the crystal structures and their symmetries (ASE [69] and PyMatGen [80]). The minimum input required to execute the workflow is the crystal structure, possibly accompanied by the definition of a magnetic order through mCIF files. More advanced options can be either

[7] https://muon-spectroscopy-computational-project.github.io/.
[8] https://training.galaxyproject.org/training-material/faqs/galaxy/histories_sharing.html.
[9] https://toolshed.g2.bx.psu.edu/.
[10] https://materialsgalaxy.stfc.ac.uk/.
[11] https://gxy.io/GTN:T00402.
[12] https://github.com/positivemuon/aiida-muon.

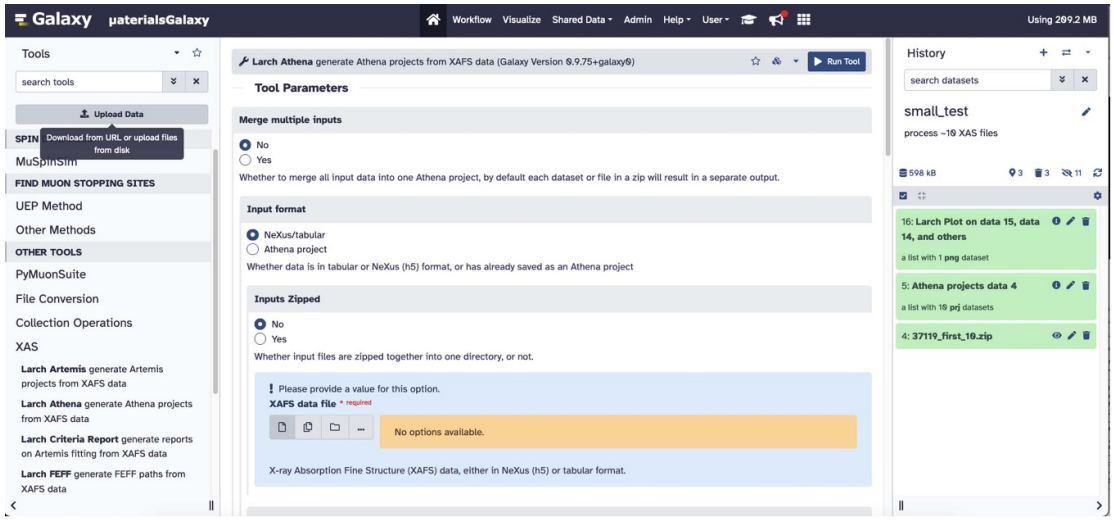

Figure 3. `materialsgalaxy` [74] main GUI. The tools' menu is on the left side, once a tool is chosen, the GUI's central panel shows the parameters associated to that tool and, as different tools are executed, their inputs and outputs are collected in the history panel on the right.

specified by the user or automatically set by the workflow. The plugin features an automated robust algorithm for the computation of the required supercell sizes and includes predefined settings for dealing with strongly correlated materials through the adoption of the DFT+U formalism [81]. This workflow is delivered within the `aiida-impuritysupercellconv`[82][13] package and used as sub-workflow in the `aiida-muon` plugin.

Currently the workflows use Quantum ESPRESSO [70] as the DFT engine underlying all simulations. However, similarly to the case of MuFinder and ASE (section 4.2), also AiiDA already provides support for tens of different DFT codes (see e.g. [83, 84], or the online AiiDA plugin registry[14]), allowing the possibility for a wider variety of electronic structures codes to be supported in the future.

In addition, to facilitate the use of the workflows, a new set of functionalities related to muon science has been added to the AiiDAlab environment [85], an open-source platform that provides an intuitive web interface for executing and sharing computational workflows performed by the AiiDA infrastructure. This is done through the `aiidalab-qe-muon`[15] plugin for the `AiiDAlab Quantum ESPRESSO` app[16], where a dedicated interface allows to interactively prepare, submit and analyze the simulations performed during the DFT+μ procedure as implemented in the already presented `aiida-muon` plugin. Using the AiiDAlab GUI, users do not need to have any programming knowledge, but can simply perform all steps (from simulation setup to result analysis) conveniently in their web browser, while the underlying AiiDA engine transparently submits DFT simulations to any local or remote HPC cluster. Once the simulations are performed, a set of panels present the results, including for instance candidate muon sites and the predicted muon polarization function, as shown in figure 4.

4.5. CalcALC

CalcALC is a Windows PC computational tool[17] developed by Francis Pratt at ISIS for simulating and interpreting muon ALC spectra of muoniated molecular radicals in both solid and liquid/gas phases using DFT. The program can also use EFG tensors calculated in closed shell diamagnetic muon systems to predict muon quadrupolar level crossing resonance (QLCR) spectra.

It can be used in two ways. One can either set up and automate Gaussian DFT calculations [71] using the STFC SCARF compute cluster or alternatively one can take the output of previous independently obtained Gaussian calculations or CASTEP magres calculations [68] as the starting point for ALC and QLCR spectral simulations. For the automated DFT calculation mode, the starting point is a molecular structure input file in pdb format. From this, the user selects muon addition and substitution sites, and a set of Gaussian jobs are prepared and submitted to the remote compute cluster. Progress of the calculations is monitored and the

[13] https://github.com/positivemuon/aiida-impuritysupercellconv.
[14] https://aiidateam.github.io/aiida-registry/.
[15] https://github.com/aiidalab/aiidalab-qe-muon/.
[16] https://aiidalab-qe.readthedocs.io/.
[17] https://shadow.nd.rl.ac.uk/calcalc/.

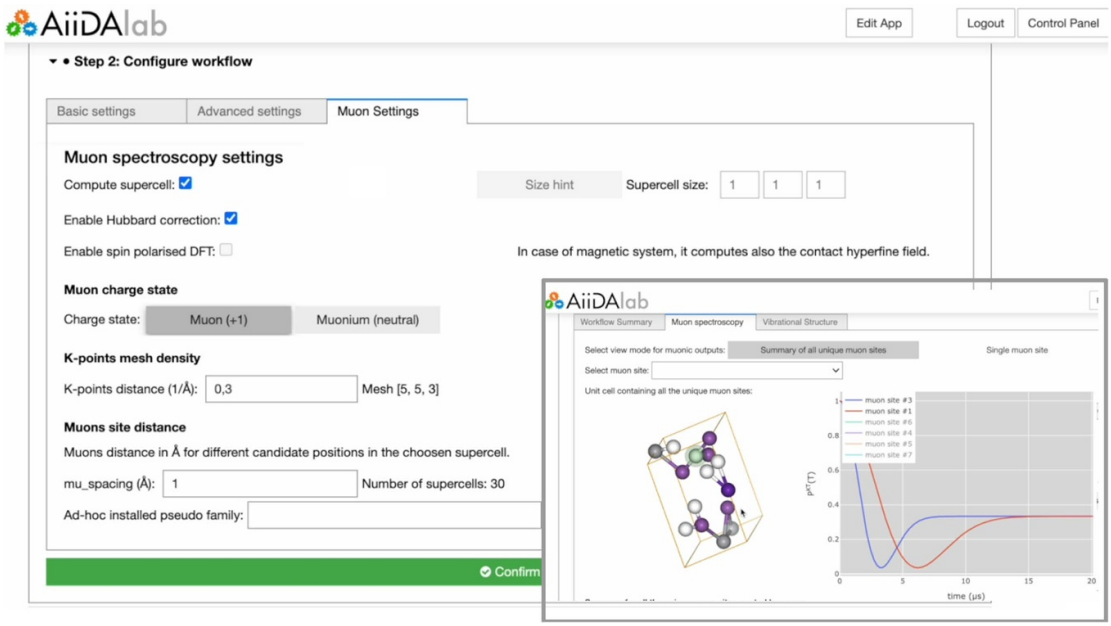

Figure 4. The GUI of the aiida-muon plugin [75, 85], which is part of the AiiDAlab Quantum ESPRESSO app. The figure shows two steps of a common user experience. The first one (in the background) is the setup phase of the calculation with its parameters; and the second one (in the foreground, bottom right) shows the results presented with two interactive visualization tools for the muon positions and the predicted polarization functions.

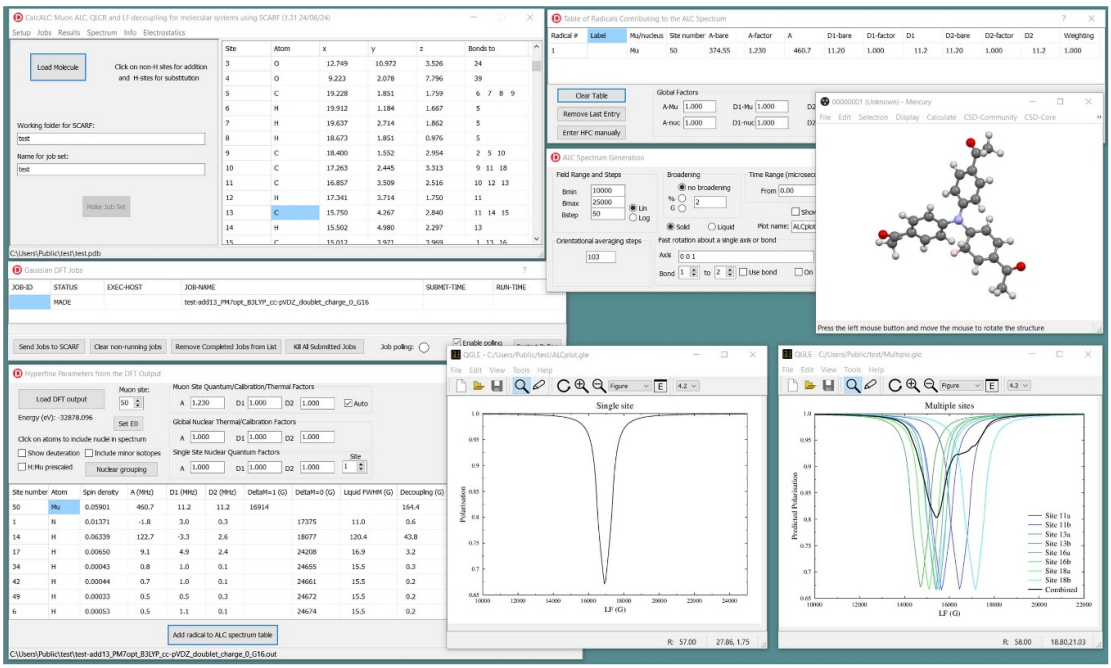

Figure 5. A screenshot of the CalcALC program being used to calculate solid-state ALC spectra for muonium addition to multiple sites on a molecule.

completed DFT output files are returned to the CalcALC host computer as the starting point for the spectral simulations.

From the single molecule Gaussian output files, the program extracts muon and nuclear hyperfine parameters or EFG parameters. It can also extract these parameters from CASTEP magres output files obtained from a calculation on a crystalline system with a periodic structure, such calculations have to be made separately before using CalcALC. For open shell systems, the radicals and strongly coupled nuclei contributing to the ALC spectrum are selected and used to define the simulated spectrum. The overall spectrum and its constituent components are finally calculated and plotted. An example screenshot of CalcALC is given in figure 5. Orientational averaging effects due to molecular rotation can be taken into

account when calculating ALC spectra, one example of this was provided in a study of corannulene [86]. A demonstration of the use of CalcALC for QLCR in a closed shell system was given by a recent study of LiTCNQ [87].

5. Conclusions

In this article, we have discussed how electronic structure calculations can be extremely useful in supporting μSR experiments by identifying the location, stability, and nature of the implanted muon site, as well as quantifying any local distortions that are introduced by the presence of the muon. These simulations can be carried out using a number of different software packages that organise the relaxation calculations, setting up the input files and processing the results. MUESR/UNDI, MuFinder, MSCP, AiiDA-muon, CalcALC are independent projects which are all being actively developed, demonstrating the vibrant activity in this field and also showcasing different software strategies. These developments are driven by a need in the muon community to be able to perform DFT+μ calculations for a large number of target materials in order to maximise the impact of an intensive experimental programme carried out by multiple research groups. This field is still in its infancy, and so many exciting advances and discoveries can be anticipated in the next few years.

Data availability statement

No new data were created or analysed in this study.

Acknowledgment

I J O, P B and R D R acknowledge financial support from PNRR MUR project ECS-00000033-ECOSISTER. M B and G P acknowledge financial support from the NCCR MARVEL, a National Centre of Competence in Research, funded by the Swiss National Science Foundation (Grant Number 205602). L L acknowledges financial support from the Ada Lovelace Centre, a STFC centre of expertise in scientific software; and from the EuroScienceGateway project, funded via the UK government's Horizon Europe funding guarantee Grant Number 10038963. J M W and L L acknowledge financial support from the STFC National Laboratories Collaborative Research Fund. T L acknowledges support from EPSRC (UK). S J B and B M H acknowledge support from UK Research and Innovation (UKRI) under the UK government's Horizon Europe funding guarantee (Grant No. EP/X025861/1).

ORCID iDs

Stephen J Blundell https://orcid.org/0000-0002-3426-0834
Miki Bonacci https://orcid.org/0000-0001-5682-0954
Pietro Bonfà https://orcid.org/0000-0001-6358-3037
Roberto De Renzi https://orcid.org/0000-0002-5015-0061
Benjamin M Huddart https://orcid.org/0000-0001-8584-105X
Tom Lancaster https://orcid.org/0000-0002-6714-4215
Leandro M Liborio https://orcid.org/0000-0003-2777-5167
Ifeanyi J Onuorah https://orcid.org/0000-0003-0448-1297
Giovanni Pizzi https://orcid.org/0000-0002-3583-4377
Francis L Pratt https://orcid.org/0000-0002-5919-3885
John M Wilkinson https://orcid.org/0000-0001-6879-7181

References

[1] Hillier A D *et al* 2022 Muon spin spectroscopy *Nat. Rev. Methods Primers* **2** 4
[2] Cox S F J 1987 Implanted muon studies in condensed matter science *J. Phys. C* **20** 3187–319
[3] Blundell S J 1999 Spin-polarized muons in condensed matter physics *Contemp. Phys.* **40** 175–92
[4] S J Blundell, R De Renzi, T Lancaster and F L Pratt ed 2022 *Muon Spectroscopy - An Introduction* (Oxford University Press)
[5] Garwin R L, Lederman L M and Weinrich M 1957 Observations of the failure of conservation of parity and charge conjugation in meson decays: the magnetic moment of the free muon *Phys. Rev.* **105** 1415–7
[6] Van de Walle C G 1990 Structural identification of hydrogen and muonium centers in silicon: First-principles calculations of hyperfine parameters *Phys. Rev. Lett* **64** 669–72
[7] Bernardini F, Bonfà P, Massidda S and De Renzi R 2013 Ab initio strategy for muon site assignment in wide band gap fluorides *Phys. Rev. B* **87** 115148
[8] Möller J S, Ceresoli D, Lancaster T, Marzari N and Blundell S J 2013 Quantum states of muons in fluorides *Phys. Rev. B* **87** 121108

[9] Brewer J H, Kreitzman S R, Noakes D R, Ansaldo E J, Harshman D R and Keitel R 1986 Observation of muon-fluorine "hydrogen bonding" in ionic crystals *Phys. Rev. B* **33** 7813–6
[10] Wilkinson J M and Blundell S J 2020 Information and decoherence in a muon-fluorine coupled system *Phys. Rev. Lett.* **125** 087201
[11] Blundell S J and Lancaster T 2023 DFT+μ: density functional theory for muon site determination *Appl. Phys. Rev.* **10** 021316
[12] Wright J D *et al* 2012 Gradual destruction of magnetism in the superconducting family $NaFe_{1-x}Co_xAs$ *Phys. Rev. B* **85** 054503
[13] Patterson B D 1988 Muonium states in semiconductors *Rev. Mod. Phys.* **60** 69–159
[14] McKenzie I 2013 The positive muon and μSR spectroscopy: powerful tools for investigating the structure and dynamics of free radicals and spin probes in complex systems *Annu. Rep. Prog. Chem. C* **109** 65–112
[15] Amato A *et al* 2014 Understanding the μSR spectra of MnSi without magnetic polarons *Phys. Rev. B* **89** 184425
[16] Vil ao R C, Vieira R B L, Alberto H V, Gil J M, Weidinger A, Lichti R L, Baker B B, Mengyan P W and Lord J S 2015 Muonium donor in rutile TiO_2 and comparison with hydrogen *Phys. Rev. B* **92** 081202
[17] Blundell S J, Steele A J, Lancaster T, Wright J D and Pratt F L 2012 A Bayesian approach to magnetic moment determination using μSR *Physica B* **30** 113–6
[18] Steele A J *et al* 2011 Low-moment magnetism in the double perovskites Ba_2MOsO_6 (M = Li, Na) *Phys. Rev. B* **84** 144416
[19] Disseler S M 2014 Direct evidence for the all-in/all-out magnetic structure in the pyrochlore iridates from muon spin relaxation *Phys. Rev. B* **89** 140413
[20] Liborio L, Sturniolo S and Jochym D 2018 Computational prediction of muon stopping sites using ab initio random structure searching (AIRSS) *J. Chem. Phys.* **148** 134114
[21] Kawaguchi K and Hirota E 1987 Diode laser spectroscopy of the ν_3 and ν_2 bands of FHF^- in 1300 cm^{-1} region *J. Chem. Phys.* **87** 6838–41
[22] Foronda F R *et al* 2015 Anisotropic local modification of crystal field levels in Pr-based pyrochlores: a muon-induced effect modeled using density functional theory *Phys. Rev. Lett.* **114** 5–9
[23] Huddart B M, Onuorah I J, Isah M M, Bonfà P, Blundell S J, Clark S J, De Renzi R and Lancaster T 2021 Intrinsic nature of spontaneous magnetic fields in superconductors with time-reversal symmetry breaking *Phys. Rev. Lett.* **127** 237002
[24] Gomilšek M, Pratt F L, Cottrell S P, Clark S J and Lancaster T 2023 Many-body quantum muon effects and quadrupolar coupling in solids *Commun. Phys.* **6** 142
[25] Errea I, Calandra M and Mauri F 2013 First-principles theory of anharmonicity and the inverse isotope effect in superconducting palladium-hydride compounds *Phys. Rev. Lett.* **111** 177002
[26] Errea I, Calandra M and Mauri F 2014 Anharmonic free energies and phonon dispersions from the stochastic self-consistent harmonic approximation: application to platinum and palladium hydrides *Phys. Rev. B* **89** 064302
[27] John Onuorah I, Bonfà P, De Renzi R, Monacelli L, Mauri F, Calandra M and Errea I 2019 Quantum effects in muon spin spectroscopy within the stochastic self-consistent harmonic approximation *Phys. Rev. Mater.* **3** 073804
[28] Deng Li, Yuan Y, Pratt F L, Zhang W, Pan Z and Bangjiao Y 2023 Two-component density functional theory study of quantized muons in solids *Phys. Rev. B* **107** 094433
[29] Sadat Riyahi N, Goli M and Shahbazian S 2023 Quantifying errors of electron-proton/muon correlation functionals through the Kohn–Sham inversion of a two-component model system *Phys. Rev. B* **108** 245155
[30] Mañas-Valero S, Huddart B M, Lancaster T, Coronado E and Pratt F L 2021 Quantum phases and spin liquid properties of 1T-TaS_2 *npj Quantum Mater.* **6** 69
[31] McClelland I, Johnston B, Baker P J, Amores M, Cussen E J and Corr S A 2020 Muon spectroscopy for investigating diffusion in energy storage materials *Ann. Rev. Mater. Res.* **50** 371–93
[32] Ito T U, Higemoto W and Shimomura K 2023 Understanding muon diffusion in perovskite oxides below room temperature based on harmonic transition state theory *Phys. Rev. B* **108** 224301
[33] Scollon M and Paul P W 2020 Free radicals formed by H atom addition to allenes as determined by muon spin spectroscopy *J. Phys. Chem. A* **124** 11086–92
[34] Martyniak A, Dilger H, Scheuermann R, Tucker I M, McKenzie I, Vujosevic D and Roduner E 2006 Using spin polarised positive muons for studying guest molecule partitioning in soft matter structures *Phys. Chem. Chem. Phys.* **8** 4723–40
[35] McKenzie I and Roduner E 2009 Using polarized muons as ultrasensitive spin labels in free radical chemistry *Naturwissenschaften* **96** 873–87
[36] Van de Walle C G and Blöchl P E 1993 First-principles calculations of hyperfine parameters *Phys. Rev. B* **47** 4244–55
[37] Yazyev O V, Tavernelli I, Helm L and Röthlisberger U 2005 Core spin-polarization correction in pseudopotential-based electronic structure calculations *Phys. Rev. B* **71** 115110
[38] Bahramy M S, Sluiter M H F and Kawazoe Y 2007 Pseudopotential hyperfine calculations through perturbative core-level polarization *Phys. Rev. B* **76**
[39] Fau S and Bartlett R J 2003 Gaussian basis sets for highly accurate calculations of isotropic hyperfine coupling constants at hydrogen *J. Phys. Chem. A* **107** 6648–55
[40] Ajith Perera S, Watts J D and Bartlett R J 1994 A theoretical study of hyperfine coupling constants *J. Chem. Phys.* **100** 1425–34
[41] Sturniolo S, Liborio L, Pratt F L, Cottrell S P, Jochym D B and Montanari B 2018 Exploring the temperature dependent solid-state ALC spectrum of the C_6H_6Mu radical with ab-initio simulation techniques JPS Conf. Proc. of the *4th Int. Conf. on Muon Spin Rotation, Relaxation and Resonance (μSR2017)* (*Sapporo, Japan, 25-30 June 2017*) vol 21 p 011036
[42] Wright J A, Peck J N T, Cottrell S P, Jablonskyte A, Oganesyan V S, Pickett C J and Jayasooriya U A 2016 Muonium chemistry at diiron subsite analogues of [fefe]-hydrogenase *Angew. Chem., Int. edn* **55** 14580–3
[43] Fan I, Chow K H, Hitti B, Scheuermann R, MacFarlane W A, Mansour A I, Schultz B E, Egilmez M, Jung J and Lichti R L 2008 Optically induced dynamics of muonium centers in si studied via their precession signatures *Phys. Rev. B* **77** 035203
[44] Shimomura K, Bakule P, Pratt F L, Ohishi K, Ishida K, Watanabe I, Matsuda Y, Nishiyama K, Torikai E and Nagamine K 2010 Pilot experiment for muonium photo ionization in gaas *J. Phys.: Conf. Ser.* **225** 012004
[45] Yokoyama K, Lord J S, Miao J, Murahari P and Drew A J 2017 Photoexcited muon spin spectroscopy: a new method for measuring excess carrier lifetime in bulk silicon *Phys. Rev. Lett.* **119** 226601
[46] Wang K *et al* 2017 Temporal mapping of photochemical reactions and molecular excited states with carbon specificity *Nat. Mater.* **16** 467–73
[47] Bakule P *et al* 2012 State-selected reaction of muonium with vibrationally excited H2 *J. Phys. Chem. Lett.* **3** 2755
[48] Bakule P, Sukhorukov O, Ishida K, Pratt F, Fleming D, Momose T, Matsuda Y and Torikai E 2015 First accurate experimental study of mu reactivity from a state-selected reactant in the gas phase: the mu + h21 reaction rate at 300 k *J. Phys. B: At. Mol. Opt. Phys.* **48** 045204

[49] Perdew J P 1985 Density functional theory and the band gap problem *Int. J. Quantum Chem.* **28** 497–523
[50] Onida G, Reining L and Rubio A 2002 Electronic excitations: density-functional versus many-body green's-function approaches *Rev. Mod. Phys.* **74** 601–59
[51] Wilkinson J M, Liborio L and Trevisanutto P 2024 (in preparation)
[52] José Uría-Álvarez A J, Esteve-Paredes J J, García-Blázquez M A and José Palacios J J 2024 Efficient computation of optical excitations in two-dimensional materials with the xatu code *Comput. Phys. Commun.* **295** 109001
[53] Umegaki I *et al* 2020 Nondestructive high-sensitivity detections of metallic lithium deposited on a battery anode using muonic x-rays *Anal. Chem.* **92** 8194–200
[54] Hampshire B V, Butcher K, Ishida K, Green G, Paul D M and Hillier A D 2019 Using negative muons as a probe for depth profiling silver roman coinage *Heritage* **2** 400–7
[55] Terada K *et al* 2014 A new x-ray fluorescence spectroscopy for extraterrestrial materials using a muon beam *Sci. Rep.* **4** 5072
[56] Terada K, Sato A, Ninomiya K, Kawashima Y, Shimomura K, Yoshida G, Kawai Y, Osawa T and Tachibana S 2017 Non-destructive elemental analysis of a carbonaceous chondrite with direct current muon beam at music *Sci. Rep.* **7** 15478
[57] Brown K L *et al* 2018 Depth dependant element analysis of pbmg1/3nb2/3o3 using muonic x-rays *J. Phys.: Condens. Matter* **30** 125703
[58] Cataldo M, Clemenza M, Ishida K and Hillier A D 2022 A novel non-destructive technique for cultural heritage: depth profiling and elemental analysis underneath the surface with negative muons *Appl. Sci.* **12** 4237
[59] Zinatulina D *et al* 2018 Electronic catalogue of muonic X-rays *EPJ Web Conf.* **177** 03006
[60] Sturniolo S and Hillier A 2021 Mudirac: a dirac equation solver for elemental analysis with muonic x-rays *X-ray Spectrom.* **50** 180–96
[61] Gill G J W, Pratt F L and Blundell S J 2023 Extending WiMDA for the data analysis of μ^-SR experiments *J. Phys.: Conf. Ser.* **2462** 012010
[62] Joseph William Gill G 2023 Site characterisation and data analysis for $\mu\pm$SR experiments *PhD Thesis* Oxford University
[63] Bonfà P, John Onuorah I and De Renzi R 2018 Introduction and a quick look at muesr, the magnetic structure and muon embedding site refinement suite *JPS Conf. Proc.* **21** 011052
[64] Martin N *et al* 2016 Magnetic ground state and spin fluctuations in mnge chiral magnet as studied by muon spin rotation *Phys. Rev. B* **93** 174405
[65] Bonfá P, Frassineti J, Maikudi Isah M M, John Onuorah I J and Sanna S 2021 Undi: An open-source library to simulate muon-nuclear interactions in solids *Comput. Phys. Commun.* **260** 107719
[66] Celio M 1986 New method to calculate the muon polarization function *Phys. Rev. Lett.* **56** 2720–3
[67] Huddart B M, Hernández-Melián A, Hicken T J, Gomilšek M, Hawkhead Z, Clark S J, Pratt F L and Lancaster T 2022 MuFinder: a program to determine and analyse muon stopping sites *Comput. Phys. Commun.* **280** 108488
[68] Clark S J, Segall M D, Pickard C J, Hasnip P J, Probert M I J, Refson K and Payne M C 2005 First principles methods using CASTEP *Z. Kristallogr.* **220** 567–70
[69] Hjorth Larsen A *et al* 2017 The atomic simulation environment-a Python library for working with atoms *J. Phys.: Condens. Matter* **29** 273002
[70] Giannozzi P *et al* 2009 QUANTUM ESPRESSO: a modular and open-source software project for quantum simulations of materials *J. Phys.: Condens. Matter* **21** 395502
[71] Frisch M J *et al* 2016 Gaussian 16 Gaussian Inc. Wallingford CT (available at: https://gaussian.com/citation/)
[72] Hourahine B *et al* 2020 DFTB+, a software package for efficient approximate density functional theory based atomistic simulations *J. Chem. Phys.* **152** 124101
[73] Sturniolo S, Liborio L, Chadwick E, Thomas J and Mudaraddi A 2023 Muspinsim: spin dynamics calculations for muon science *J. Phys.: Conf. Ser.* **2462** 012017
[74] Afgan E *et al* The Galaxy Community 2022 The Galaxy platform for accessible, reproducible and collaborative biomedical analyses: 2022 update *Nucl. Acids Res.* **50** W345–51
[75] Onuorah I J *et al* 2025 Automated computational workflows for muon spin spectroscopy *Digital Discovery* **4** 523–38
[76] Onuorah I J *et al* 2025 positivemuon/aiida-muon: v1.0.3 *Zenodo* (https://doi.org/10.5281/zenodo.14594493)
[77] Pizzi G, Cepellotti A, Sabatini R, Marzari N and Kozinsky B 2016 AiiDA: automated interactive infrastructure and database for computational science *Comput. Mater. Sci.* **111** 218–30
[78] Huber S P *et al* 2020 AiiDA 1.0, a scalable computational infrastructure for automated reproducible workflows and data provenance *Sci. Data* **7** 300
[79] Uhrin M, Huber S P, Yu J, Marzari N and Pizzi G 2021 Workflows in AiiDA: engineering a high-throughput, event-based engine for robust and modular computational workflows *Comput. Mater. Sci.* **187** 110086
[80] Ping Ong S *et al* 2013 Python materials genomics (pymatgen): a robust, open-source python library for materials analysis *Comput. Mater. Sci.* **68** 314–9
[81] Cococcioni M and de Gironcoli S 2005 Linear response approach to the calculation of the effective interaction parameters in the LDA + U method *Phys. Rev. B* **71** 035105
[82] Onuorah I J *et al* 2025 positivemuon/aiida-impuritysupercellconv: v1.0.1 *Zenodo* (https://doi.org/10.5281/zenodo.14594496)
[83] Huber S P *et al* 2021 Common workflows for computing material properties using different quantum engines *npj Comput. Mater.* **7**
[84] Bosoni E *et al* 2024 How to verify the precision of density-functional-theory implementations via reproducible and universal workflows *Nat. Rev. Phys.* **6** 45–58
[85] Yakutovich A V *et al* 2021 AiiDAlab - an ecosystem for developing, executing and sharing scientific workflows *Comput. Mater. Sci.* **188** 110165
[86] Gaboardi M, Pratt F, Milanese C, Taylor J, Siegel J and Fernandez-Alonso F 2019 The interaction of hydrogen with corannulene, a promising new platform for energy storage *Carbon* **155** 432
[87] Berlie A, Pratt F L, Huddart B M, Lancaster T and Cottrell S P 2022 Muon-nitrogen quadrupolar level crossing resonance in a charge transfer salt *J. Phys. Chem. C* **126** 7529–34